POAC'17
Busan, KOREA

Proceedings of the 24th International Conference on
Port and Ocean Engineering under Arctic Conditions
June 11-16, 2017, Busan, Korea

Flexural Strength of Ice Reconstructed from Field Tests with Cantilever Beams and Laboratory Tests with Beams and Disks

Aleksey Marchenko[1], Marina Karulina[2], Evgeny Karulin[2], Peter Chistyakov[3], Alexander Sakharov[3]
[1] The University Centre in Svalbard, Longyearbyen, Norway
[2] Krylov State Research Centre (KSRC), St. Petersburg, Russia
[3]Lomonosov Moscow State University, Moscow, Russia

ABSTRACT

More than 60 in-situ tests have been performed since 2010 to determine flexural strength of sea ice and freshwater ice in North-West Barents Sea, Spitsbergen Fjords, and fresh water lake near Longyearbyen in Spitsbergen. Ice thickness in the tests varied from 20 cm to 80 cm. Dependencies of flexural strength on temperature and salinity, averaged over ice thickness, were found. Results of in-situ, cantilever-beam tests are analyzed and compared with results of laboratory tests of 3-point bending of ice beams and central loading of ice discs.

KEY WORDS: Sea ice, Flexural strength, Cantilever beam, Liquid brine

INTRODUCTION

Flexural strength of ice characterizes capacity of ice to resist pure bending deformations without failure. Flexural strength of materials is measured in standard tests of different types, including most typical 3- and 4-point-bend tests and tests with cantilever beams. In these tests, beam samples have dominant principal stress oriented along the beam axes while absolute values of the other principal stresses are small over the beam volume, excluding the beam edges where the stress concentration occurs. In 3- and 4-point-bend tests, the stress concentration also occurs at the points of loading and beam support. In cantilever-beam tests, the stress concentration occurs near the beam root. Local failure of material in places of stress concentration may not influence global failure of a beam, but its influence on flexural strength and displacements of the beam can be significant. Information about the displacements is used to determine effective elastic characteristics of a beam.

Flexural strength tests with beams are used for concrete (GOST 10180-90), ice (ISO 19906) and other brittle materials. In the case of ceramics, it is shown by comparing tests results with results of finite element modeling that tests with central loading of discs can be used instead of beam tests (Moskvichev et al., 2002). Recommendations in ISO 19906 are "the preferred

cantilever beam test, in which the in-situ ice cover is cut along three sides and loaded [at] the free end of the cantilever". Russian documents on Site Investigation of the Continental Shelf for Offshore (2004) accept tests with ice disks for determination of flexural strength of ice. The analytical formula of Timco and Brien (1994) approximating the dependence of flexural strength on the liquid brine content is based on the results of tests with beams. Tests with disks were performed during AARI expeditions in Barents Sea during the time period of 1996-2006 (Krupina and Kubyshkin, 2007).

In the present paper, we describe the results of in-situ tests with ice cantilever beams (FST1) performed since 2009 in Spitsbergen fjords and North-West Barents Sea. These results are compared with the results of laboratory tests performed on 3-point bending of beams (FST2) and tests with central loading of ice discs (FST3).

ORGANIZING OF FIELD AND LABORATORY TESTS

Figure 1 shows sketches of flexural-strength tests to describe the flexural behavior of ice during three types of tests. FST1 is performed on a floating ice in the field and laboratory ice tank. An ice beam is prepared by making three vertical trenches over entire ice thickness (Figure 1a). The trenches should be wide enough to avoid the interaction of the cantilever beam faces with surrounding ice when the beam is loaded by a force F, applied at the free end of the beam. Vertical holes are drilled near the beam roots to avoid stress concentration. Nevertheless, some stress concentrations are created around the holes due to the beam bending, influencing the test results. Length of the beam is approximately 6 times the beam width and ice thickness. Snow is not removed from the surface of the beam to avoid any influence on the beam buoyancy forces.

The following equipment was fabricated and installed for the in-situ tests (Figure 2):

- Steel loading rig transferring force from immovable ice cover to the loaded ice beam;
- Steel loading rig for the mounting of the displacement sensor;
- Steel loading frame transferring force from Single-Acting Cylinder to the ice beam in upward direction;
- Hydrosystem (Single-Acting Cylinder RC-154, Electric Pump ZE-Series);
- Generator (3-phase, 400 V);
- Load cell NTT C8S- 82-1-100kN to measure compressive load;
- PCM 620 - Bi-Directional S-Type Load Cell, 20 kN to measure tensile load;
- Displacement sensor ASM WS 1007287917
- Data Logger Campbell Scientific CR1000.

Records of the load F and the displacement δ of the loaded end of the beam were monitored and recorded during a test at a sampling frequency of 50 Hz. Tests were performed on land-fast ice in Ice Fjord and Van Mijen Fjord in Spitsbergen, on drifting ice in North-West Barents Sea, and on freshwater lake ice near Longyearbyen, Spitsbergen.

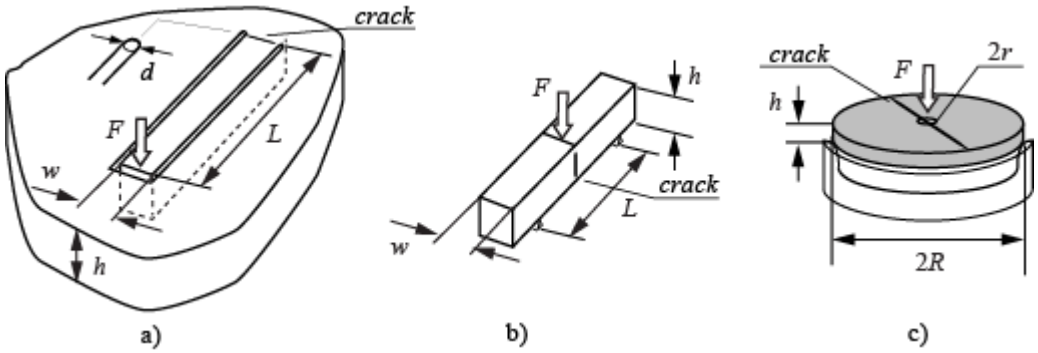

Figure 1. Schematic sketches of flexural-strength test with a cantilever beam (FST1) (a), 3-point-bend test with a beam (FST2) (b), and test with central loading of a disc (FST3) (c).

The following equipment was used in the laboratory tests FST2 and FST 3 (Figure 3):

- Compression rig Knekkis with maximal load 100 T mounted in the cold laboratory of UNIS;
- Deflectometer Epsilon, Model 3540-004M-ST, travel 4.00 mm;
- HBM C9C Force transducer, 5 kN;
- Bearers for tests FST2 and FST3;

Displacements δ of beams and discs were measured at a sampling frequency of 50 Hz. The load during FST2 was measured at a sampling frequency of 20 Hz. The load in FST3 was measured by HBM Force transducer at a sampling frequency of 50 Hz.

a) b) c)

Figure 2. In-situ flexural strength tests on sea ice with downward (a) and upward (b) loading, Flexural strength test on freshwater lake ice (c).

Several tests FST3 were performed in-situ on drifting ice in North-West Barents Sea (Figure 3c). In this case, square ice plate is placed on a circular support having a diameter of 24 cm, which is hidden below an ice plate in Figure 3c. The load was applied on the ice and measured with the same equipment as in FST1.

STRUCTURE OF ICE SAMPLES IN LABORATORY AND FIELD TESTS

Figure 4 shows the internal structure of ice samples taken from the ice subjected to flexural strength tests in laboratory and in-situ tests. Natural sea ice has columnar structure over almost entire ice thickness. Surface ice layer may have granular structure when it is formed from the mixture of melt snow and seawater. Brine inclusions exist between and inside the grains. Grain boundaries of sea ice are not so sharp as in freshwater lake ice. The grain sizes are similar in the freshwater and seawater ice. Laboratory ice having a salinity less than 3-5 ppt is grown in a 1-m-by-0.5-m ice tank at UNIS from a mixture of seawater and freshwater having a total salinity around 9 ppt. Granular structure of the laboratory ice depends on the distance from the tank walls, because the directions of ice growth are different in different places of the tank.

a) b) c)

Figure 3. Laboratory tests on 3-point-bend test(FST2) of an ice beam (a), central loading of an ice disc (FST3) (b). In-situ test on central loading of ice disc (FST3) (c).

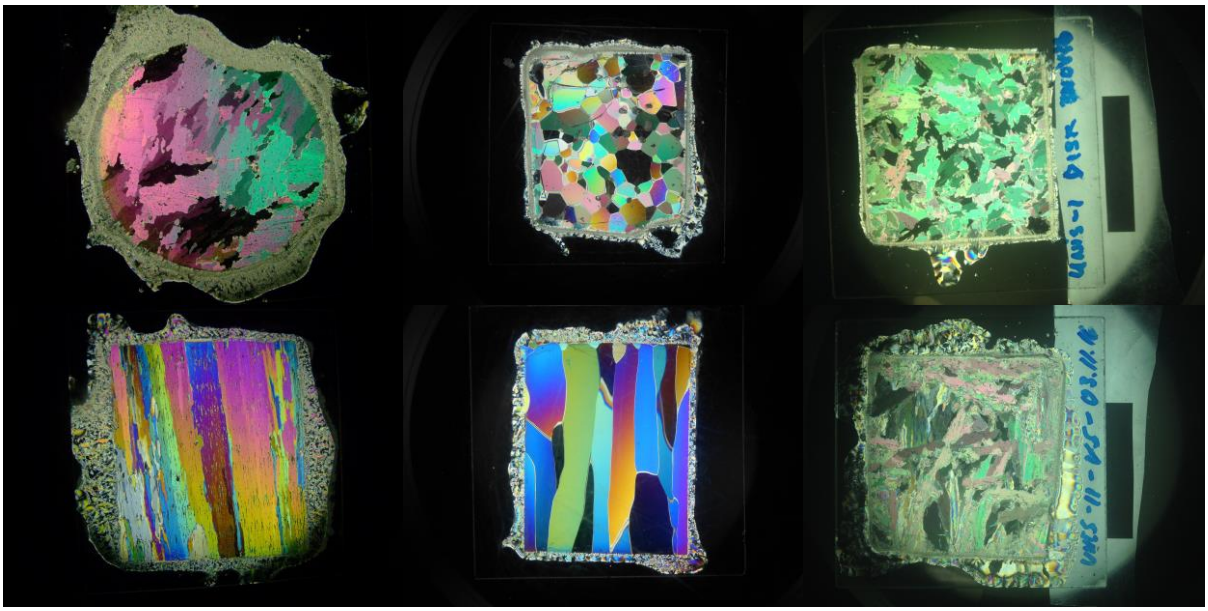

Figure 4. Thin sections of sea ice (left column), lake freshwater ice (middle column) and laboratory ice (right column). Upper and down panels show vertical and horizontal sections respectively.

Sea ice thickness during the FST1 tests was in the range of h=30-75 cm. The thickness of

freshwater lake ice during the FST1 tests was in the range of h=30-40 cm. In the present paper, we report the results of 45 FST1 tests performed on sea ice and FST1 14 tests performed on fresh lake ice. Displacement was measured only in 14 FST1 tests performed on sea ice, and in all tests performed on freshwater lake ice. Two FST1 tests were performed in the ice tank on saline ice with cantilever dimensions h=13 cm, w=11 cm and L=55 cm. Geometrical characteristics of the ice beams in the FST2 tests were h=12 cm, w=6.5-12 cm, and L=46-66 cm. In the present paper, we report the results of 6 FST2 tests performed on saline ice beams. The thickness of ice discs in the laboratory FST3 tests was in the range of h=1-1.5 cm, and the diameter of the disks was $2R$=14 cm. The load was applied over the metal disk with diameter $2r$=1 cm. In-situ tests were performed with rectangular plates of sea ice with thickness h=4-5 cm. The load was applied over the plastic disk with diameter $2r\approx$4 cm. In the present paper we report the results of 12 FST3 tests performed on saline ice in the laboratory, and 4 in-situ FST3 tests performed on sea ice.

RESULTS OF TESTS

Figure 5 shows examples of load-displacement curves during tests in the laboratory and the field. All FST1 tests demonstrated brittle behavior of the ice with failure by a vertical crack near the beam root. The linear load-displacement curves demonstrate elastic behavior of ice in these tests (Figure 5a). The flexural strength and effective elastic modulus are calculated using the following formulae

$$\sigma_f = \frac{6F_{\max}\cdot L}{wh^2},\quad E = \frac{F_{\max}}{\delta_{\max}}\frac{4L^3}{h^3 w}, \tag{1}$$

where $F_{\max}$ is the maximal load, and $\delta_{\max}$ is the displacement of the loading point of beam at the moment of maximal load. The length L is measured between the point of the loading and the crack near the beam root. Representative test duration is t^*=1 s. The strain rate estimated with formula $e=(\delta_{\max}/Lt^*)$ varies between 10^{-4}s^{-1} and 10^{-3}s^{-1}.

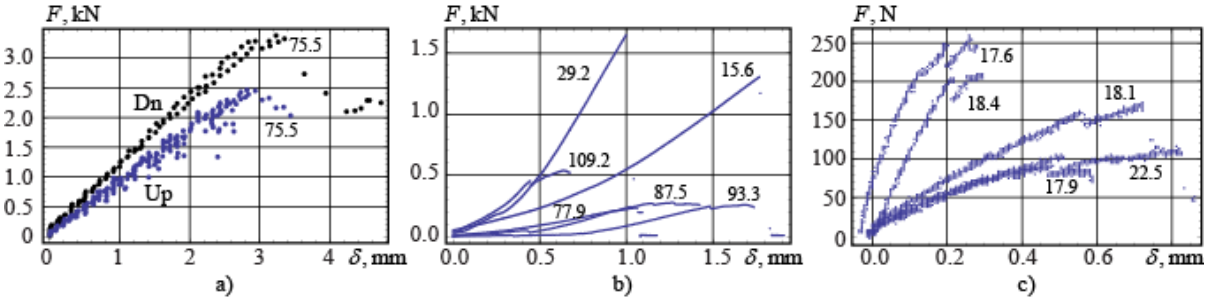

Figure 5. Examples of load-displacement curves during the in-situ tests FST1(a), laboratory tests FST2 (b) and FST3(c). Liquid brine content of ice in ppt is written in the figures.

The dependence of load F with respect to displacement of a beam near the loading point δ is not linear during the tests FST2 (Figure5b). The nonlinear behavior is probably related to local deformations of the ice beam near the loading point and near the contact points of the supports. This introduces error in measurement of the displacement. The flexural strength from a FST2 test is calculated with the following formula:

$$\sigma_f = \frac{3F\cdot L}{2wh^2}, \tag{2}$$

where L is the distance between the supports (Figure 1b). Loading duration is t^*=15 s. Maximal measured displacements are about 1 mm. Effective strain rate estimated with formula $e=2\delta_{max}/Lt^*$ is around $2.5\cdot10^{-4}$ s^{-1}.

The dependence of load F with respect to displacement of a disc near the loading point δ is not linear during the tests FST3 (Figure5c). The nonlinear behavior is probably related to creep deformations of the disc due to in-plane compression near the loading point. The function $F(\delta)$ has two local maxima separated by a discontinuity. The first maxima is related to the formation of bending crack which is probably is not going through the disc thickness. The second maxima is probably related to the beam failure due to the compression in surface layer. Similar scenario is observed in the tests with fixed ends beams (Sodhi, 1998; Sakharov et al, 2015; Karulina et al, 2016). Nonlinear dependence $F(\delta)$ demonstrates inelastic behavior of the disc under the load. Therefore the elastic theory can be used for the calculation of the effective elastic modulus of the disc only in the initial period of the loading. The flexural strength is calculated with the formula (Timoshenko and Woinowsky-Krieger, 1959)

$$\sigma_f = \frac{3F}{8\pi h^2}\left[4-(1-\nu)\left(\frac{r}{R}\right)^2-4(1+\nu)\ln\left(\frac{r}{R}\right)\right], \quad (3)$$

where ν is the Poisson's ratio. The Poisson's ratio of sea ice depends on the temperature and strain rate and has representative value of 0.33 (Timco and Weeks, 2010). We use the representative value ν=0.33 in formula (3). Loading duration is t^*=10 s. Maximal measured displacements are about 0.25 mm. The strain rate estimated with formula $e=\delta_{max}/Rt^*$ is around $3.5\cdot10^{-4}$ s^{-1}.

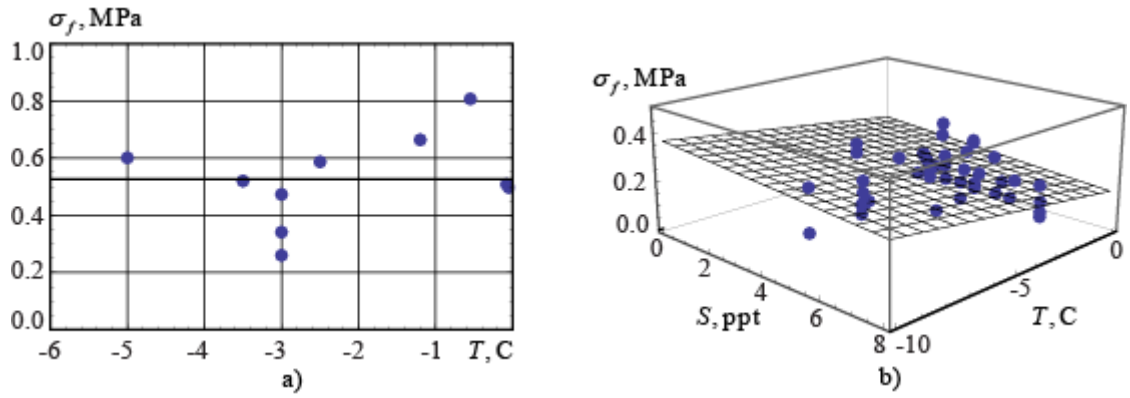

Figure 6. Flexural strength versus temperature of lake freshwater ice (a), and flexural strength versus temperature and salinity of sea ice (b).

Figure 6a shows plots of flexural strength versus temperature of freshwater lake ice as obtained from FST1 test. Mean value of the flexural strength is 0.53 MPa. It is much lower than the values given by Timco and O'Brien (1994) for ice temperatures below -4.5^{o}C. Figure 6b shows plots of flexural strength of sea ice versus the ice temperature and salinity averaged over the ice thickness, as obtained from the FST1 tests. Mean value of the flexural strength is 0.244 MPa. It is very close to the values of the flexural strength of 0.249 MPa and 0.254 MPa obtained from similar in-situ tests performed in the North-East and South-East Barenst Sea (Krupina and Kubyshkin, 2007). Frederking and Hausler (1978) performed 11 in-situ FST1

tests in the Ice Fjord, Spitsbergen. The ice thickness during those tests was around 40 cm. In their tests the ratio L/h varied from 8.6 to 29.4 with mean value 13.64. They found the mean value of the flexural strength of 0.39 MPa. The high value of the flexural strength is attributed to the influence of the buoyancy forces on the deflected shape of long beams. In case when $L/h<6$, the influence of the buoyancy forces on the beam deflected shape is not significant (see, e.g., Karulina et al., 2010).

The plane in Figure 6b is described by the equation

$$\sigma_f = 0.236 - 0.095 \cdot S - 0.0134 \cdot T. \quad (4)$$

In standard approximation, the flexural strength is expressed as a function of the liquid brine content (Frankenstein and Garner, 1967)

$$\nu_b = S\left(\frac{49.185}{|T|} + 0.532\right), \quad -0.5^{\circ}\mathrm{C} \geq T \geq -22.9^{\circ}\mathrm{C}. \quad (5)$$

Results of in-situ FST1 tests are plotted on a plane $(\sqrt{\nu_b}, \sigma_f)$ in Figure 7a by blue points. Pink and blue lines are described by the equation

$$\sigma_f = A \cdot \exp\left(-B\sqrt{\nu_b}\right). \quad (6)$$

Timco and O'Brien (1994) proposed to use coefficients A=1.76 and B=5.88 (pink line). The best-fit line for the present data by formula (6) is obtained with coefficients of A=0.45 and B=2.2 (blue line). Standard deviations of the data from the approximations given by formula (4) and formula (6) are of the same order of magnitude.

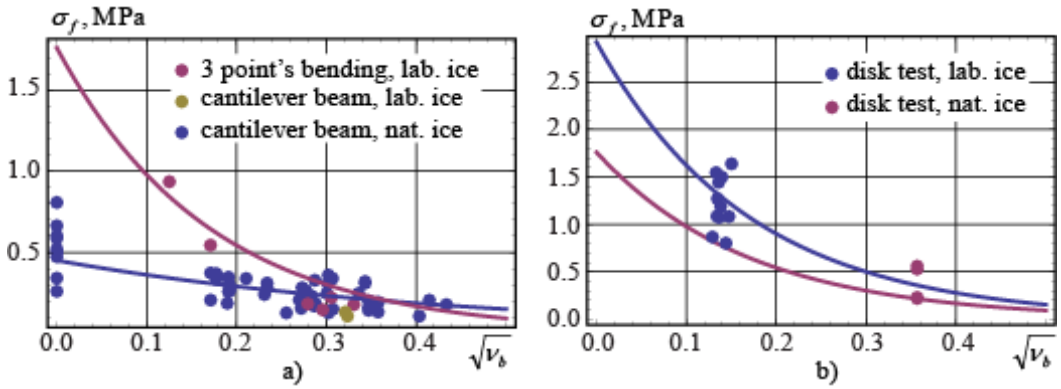

Figure 7. Flexural strength of freshwater and saline ice from in-situ and laboratory tests with beams versus the liquid brine content (a). Flexural strength of saline ice from in-situ and laboratory tests with discs versus the liquid brine content (b).

Pink points in Figure 7a are found from the tests FST2. They fit the approximation given by formula (6) better with the coefficients proposed by Timco and O'brien (1994). Green points in Figure 7a are obtained from the tests FST1 performed in the ice tank.

Blue and pink points in Figure 7b are found, respectively, from the laboratory and in-situ FST3 tests. The pink line in Figure 7b corresponds to the pink line in Figure 7a. The blue line in Figure 7b is described by formula (6) with coefficients A=2.769 and B=5.88. According to this approximation the flexural strength calculated from the tests FST3 is 1.66 times greater than the flexural strength calculated with the formula of Timco and O'Brien (1994). Krupina and Kubyshkin (2007) found that flexural strength obtained from the FST3 tests is greater by more than in 5 times than the flexural strength obtained from the FST1 tests. We think that this difference can be attributed to the difference in temperature: tests with discs were performed at a lower ice temperature than the tests with floating cantilever beams.

Figure 8a shows plots of effective elastic modulus of freshwater ice calculated with the second formula (1) versus ice temperature. There is big spread of the data around the mean value $\langle E_{eff}\rangle \approx 2.94$ GPa. Figure 8b shows plots of effective elastic modulus of sea ice calculated with the second formula (1) versus the liquid brine content. The mean value is equal to $\langle E_{eff}\rangle \approx 1.26$ GPa. Black line shows the approximation of effective elastic modulus as proposed Vaundrey (1977)

$$E_{eff} = 5{,}31 - 0.436\sqrt{\nu_b}\,, \tag{7}$$

where ν_b is substituted in ppt, and E_{eff} is found in GPa.

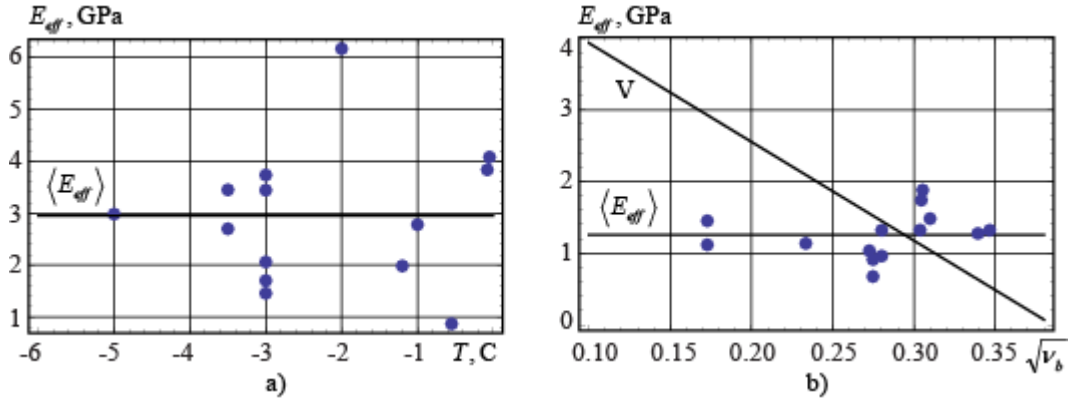

Figure 8. Elastic modulus of lake freshwater ice versus the temperature (a). Elastic modulus of sea ice versus the liquid brine content (b).

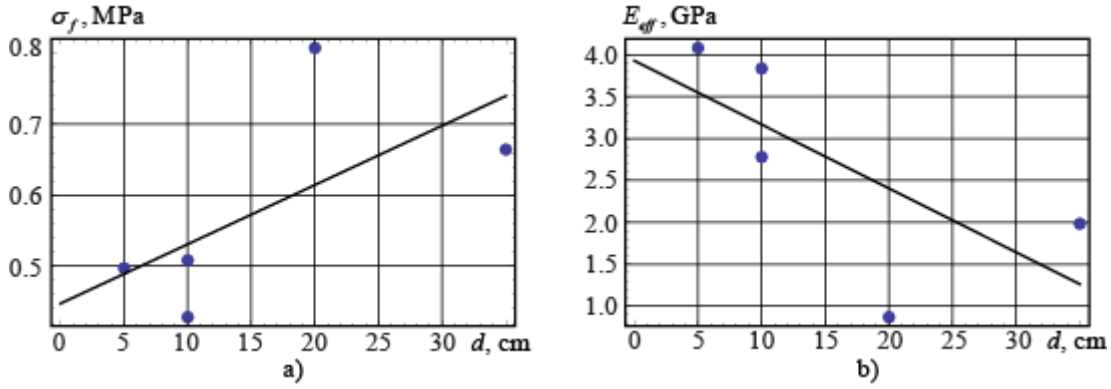

Figure 9. Flexural strength (a) and elastic modulus (b) of lake freshwater ice versus the diameter of the holes near the beam roots.

Figure 9 shows the dependence of flexural strength and effective elastic modulus of fresh ice as obtained from in-situ FST1 tests on diameters *d* of holes drilled near the beam roots. The tests were performed on the same ice and at the same time. The flexural strength and effective elastic modulus are calculated with formulas (1). We discovered an increase in flexural strength and a decrease of the elastic modulus with an increase in diameter of holes.

$$\sigma_f = 0.447 + 0.835 \cdot d \ , \ \left\langle E_{eff} \right\rangle = 3.927 - 7.615 \cdot d \ , \tag{8}$$

where *d* is measured in meters, σ_f is calculated in MPa, and $\langle E_{eff} \rangle$ is calculated in GPa.

CONCLUSIONS

Tests with cantilever FST1 beams provide most useful information about the flexural strength and the effective elastic modulus of floating ice. It is attributed to pure brittle failure of ice cantilevers in the tests and a linear dependence between load and displacement during a test. We discovered that flexural strength of sea ice in North-West Barents Sea and Spitsbergen Fjords is of the same magnitude to those in North-east and South-East regions of the Barents Sea. Flexural strength obtained from in-situ FST1 tests is less than the strength prescribed by the formula of Timco and O'Brien (1994). An effect of ice temperature and salinity on the effective elastic modulus is not found. There is an influence of diameter of holes near the beam roots on the flexural strength and effective elastic modulus as obtained from FST1 tests. An increase in diameter increases the flexural strength and decreases the effective elastic modulus.

ACKNOWLEDGEMENTS

The authors wish to acknowledge the support of the Research Council of Norway through the Center for Sustainable Arctic Marine and Coastal Technology (SAMCoT). Authors thank Dr. Devinder Sodhi for the valuable comments to the paper.

REFERENCES

Frankenstein, G.E., Garner, R., 1967. Equations for determining the brine volume of sea ice from -0.5 to -22.9°C. J. Glaciology, 6(48), 943-944.

Frederking, R.M.W., Hausler, F., 1978. The flexural behavior of ice from in situ cantilever beam tests. Proc. of the IAHR Symposium on Ice Problems, Lulea, Vol. 1, 197-215.

International Standard (ISO 19906), 2010. Petroleum and natural gas industries – Arctic offshore structures. ISO copyright office, Geneva.

GOST 10180-90. Concretes. Methods for strength determination using reference specimens. 1991-01-01. (in Russian)

Karulina, M., Karulin, E., Dmitriev, D.S., Alexeev, Y.N., 2010. Procedural peculiarities of the model ice properties determination. Proc. of the 20the IAHR Symposium on Ice, Lahti, Finland, paper 57.

Karulina, M., Marchenko, A., Sakharov, A., Karulin, E.,Chistyakov, P., 2016. Experimental Studies of Fracture Mechanics for Various Ice Types. Proc. of the 23rd IAHR Symposium on Ice, Ann Arbor, Michigan, paper 4869357.

Krupina, N.A., Kubyshkin, N.V., 2007. Flexural strength of drifting level first-year ice in the Barents Sea. Proceedings of ISOPE, Lisbon, Portugal, 625-632.

Moskvichev, V.V., Makhutov, N.A., Chernyaev, A.P., et al., 2002. Fracture toughness and mechanical properties of construction materials for technical systems. Nauka: Novosibirsk, 334 p.

Sakharov, A., Karulin, E., Marchenko, A., Karulina, M., Sodhi, D., Chistyakov, P., 2015. Failure envelope of the brittle strength of ice in the fixed-ends beam test (two scenarios). POAC15-00230, Trondheim, Norway

Site Investigation on the Continental Shelf for Offshore. СП 11-114-2004.

Sodhi, D.S., 1998. Vertical penetration of floating ice sheets. International Journal of Solids and Structures, 35 (31-32): 4275-4294.

Timco, G.W., O'Brien, S.O., 1994. Flexural strength equation for sea ice. Cold Regions Science and Technology. 22, 285-298.

Timco, G.W., Weeks, W.F., 2010. A review of the engineering properties of sea ice. Cold Regions Science and Technology. 60, 107-129.

Timoshenko, S., Woinowsky-Krieger, S., 1959. Theory of plates and shells. 2nd ed., McGraw-Hill, New York, USA.

Vaudrey, K.D., 1977. Ice engineering – study of related properties of floating sea-ice sheets and summary of elastic and viscoelastic analyses. (Technical Report Naval Construction Battalion Center) Civil Engineering Laboratory, Port Hueneme, CA